1 Introduction

As one of the most vibrant areas in the communication field, wireless communication has been going through rapid development. On the other hand, there has been an explosive increase in demand for tetherless access in more and more scenarios. The Internet of Things (IoT), for instance, is an important development stage of information age. The vision of IoT is to achieve "Internet of Everything"; the key to the realization of the goal is to build a fully connected multiuser network that can be applied to diversified communications. As IoT applications are extending to more and more scenarios, common wireless communication techniques using electromagnetic (EM) waves are becoming dissatisfactory in both coverage and connectivity. EM waves experience high levels of attenuation due to absorption by a natural medium, such as soil, rock, and water, which leads to its inability to transmit in some challenging environments (underground, deep mine, mountain, rock, ice, tunnel, underwater, forest, . . .) as well as restrictions to the development of IoT.

To overcome this difficulty, deep penetration techniques, such as magnetic communications (MC), have brought solutions to these transmission problems. The so-called MC makes use of the time-varying magnetic field produced by the transmitting antenna, so that the receiving antenna receives the energy signal by mutual inductance. Researches show that the penetrability of the MC system depends on the magnetic permeability of the medium. Because the magnetic permeability of the layer, rock, ice, soil, and ore bed is close to the air, channel conditions bring less effects to magnetic transmission than electric transmission. Therefore, the communication network based on deep-penetrating magnetic induction (MI) can expand the perception ability and sensing range of information technology effectively, which can be applied to complex environments, such as underground, underwater, tunnel, mountain, rock, ice, and forest. We can conclude that the network construction of IoT based on MC is of great value and can be regarded as one of the reliable technologies to improve the connectivity of a wireless network.

The deep-penetrating MC technology is based on the principle of mutual inductance of the magnetic field. The alternating magnetic field is generated by the transmitting coil, and the receiving terminal also uses the coil antenna to measure the mutual inductance of the time-varying magnetic field in the space to obtain the information encoded in the time-varying signal (Fig. 1.1). In MC technology, in order to achieve reliable long-distance penetrating transmission, the sensitivity of the receiving antenna is usually required to reach the pT (pico Tesla) level. In addition, the performance

https://doi.org/10.1017/9781108674843.003 Published online by Cambridge University Press

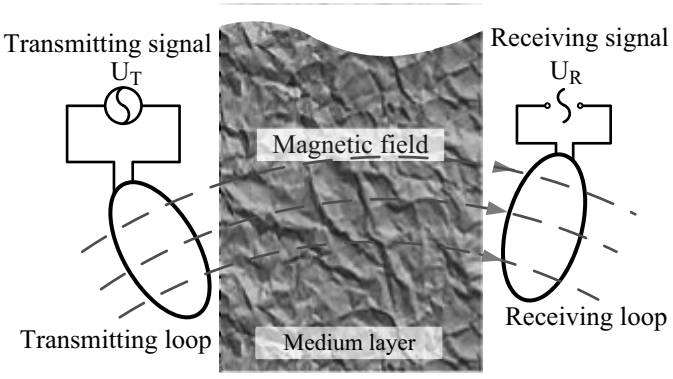

Figure 1.1 Wireless magnetic communication

optimization of the transmitter circuit in MC, antenna design, and receiving signal noise filtering are very challenging technical aspects.

Fundamental EM field and circuit theories for MC are included in this chapter. Advanced MC theory and latest MI applications are discussed in the following chapters.

1.1 Magnetic Communication and Wireless Communication

In the last two decades, driven by a wealth of theoretical development and practical requirement, many kinds of communication technologies under different situations drew the attention of research community. At present, the mainstream communication technologies include acoustic communication, optical waves communication, EM wave communication, and MC. This chapter covers the subject of the differences between MC and wireless communication.

1.1.1 The Comparison between Magnetic Communication and Other Wireless Communications

For most challenging environments mentioned in the beginning, there are no wireless communications deployment attempts before IoT applications. On the other hand, other wireless communication technologies are not able to provide reliable coverage and connectivity in such environments. Take underground mine for example, EM-wave-based wireless communication can only support a semi-wireless system, in which the links between the surface and underground are wired. Such a system is vulnerable, especially in a disaster situation.

However, in an underwater environment, many wireless communication technologies have been studied for both industry and military demands. The majority of the work on underwater communication is mainly based on acoustic communication, while it exhibits high propagation delays along with very low data rates, and highly

https://doi.org/10.1017/9781108674843.003 Published online by Cambridge University Press

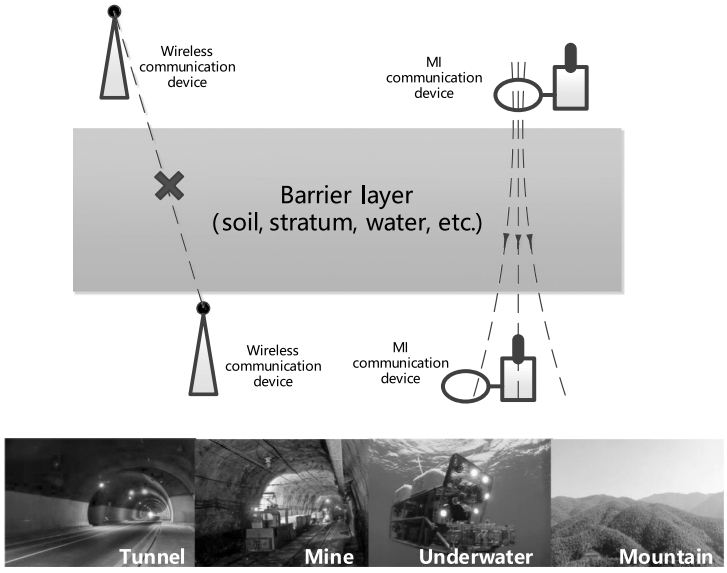

Figure 1.2 Communication scenarios under rugged environment

environment-dependent channel behavior. The highly environment-dependent channel behavior in underwater communication is caused by complex multipath fading, prevalent Doppler effects, and significant variation of these properties due to temperature, salinity, or pressure [1]. Optical waves do not suffer from high attenuation but experience multiple scattering of light, which results in inter-symbol interference and short transmission range [2]. Moreover, the transmission of optical signals requires high precision in pointing the narrow laser beams. Traditional wireless communication techniques using EM waves encounter three major problems: high path loss, dynamic channel condition, and large antenna size [3]. EM waves experience high attenuation that severely limits the achievable communication range. To increase the communication range, large antennas are required for low-frequency EM communication, which is not practical for small underwater vehicles and robots.

To sum up, the penetration ability of the traditional approaches is relatively weak, leading to propagation difficulties in a challenging environment, such as underground, deep mine, mountain area, terrane, tunnel, underwater, and forests, as shown in Fig. 1.2.

1.1.2 Benefits of Magnetic Communication

Magnetic communication is a promising alternative technique providing solutions for the mentioned problems. It utilizes the transmitting antennas to generate a time-varying magnetic fields in the medium, thus enabling the receiving antennas to receive the energy signal in a sense of mutual inductance. Our research shows that the dielectric penetration performance of the MC system depends mainly on the magnetic conductivity of the medium.

https://doi.org/10.1017/9781108674843.003 Published online by Cambridge University Press

Using MI could have several benefits. One of these benefits is that dense media (such as soil and water) cause little variation in the rate of attenuation of magnetic fields from that of air, since the magnetic penetrability for each of these materials is almost the same [4]. Although generally unfavorable for open-air communication since the magnetic field strength falls faster than that in EM waves, the reduction in signal loss caused by propagation through soil compensates for this in the underground scenario.

Another favorable property of MI is that since the magnetic field is generated in the near field, it is non-propagating [4], which means that multipath fading is not a problem for MC. Moreover, since communication is achieved by coupling in the non-propagating near field, a transmitting device can detect the presence of any active receivers via the induced load on the coil. This property may provide valuable information for protocols, acting as a type of acknowledgement that the transmission was sensed by a remote device.

In an MC system, the antenna design is accomplished with the use of a coil of wire for both transmission and reception. The strength of the magnetic field produced by a given coil is proportional to the number of turns of wire, the cross-sectional area of the coil, and the magnetic permeability of any material placed in the core of the coil. The use of wire coils for MI transmission and reception represents a substantial benefit over the use of antennas for propagating EM waves. Low frequencies necessary for the propagation of EM waves mean that large antennas are necessary for reasonable efficiency, which obviously conflicts with the necessity that underground sensors remain small.

We take the underwater scenario, for instance, as shown in Table 1.1. Although the bandwidth of the MI system is smaller than that of the EM wave system, MC provides a longer transmission range. MC also has the advantage that its performance is not influenced by the properties of the medium.

Based on the advantages discussed above, an MC network can effectively expand the awareness and perception of the network. It has a good performance even in some harsh scenarios with many natural mediums or medium boundaries, such as underground, underwater, tunnels, massif, rock stratum, ice layer, and forest. The MI system enables a reliable and stable communication in some challenging environments instead of the EM system.

1.1.3 Applications of Magnetic Communication

Different from the traditional EM communication systems, the transmitting antenna of an MC system is equivalent to a magnetic dipole, which almost does not generate an electric field. Hence, the MI carrier is not a propagating wave, and it can be regarded as a quasi-static magnetic field generated in the air. So, the MI signals are free from the influence of multipath propagation compared with ordinary wireless signals. Due to the fact that the permeability of soil and water is close to that of air, MI signals

https://doi.org/10.1017/9781108674843.003 Published online by Cambridge University Press

Table 1.1 Comparison of underwater MI, EM, acoustic, and optical communications

Communication paradigm	Propagation speed	Data rates	Communication ranges
MI	3.33×10^8 m/s	Mb/s	10–100 m
EM	3.33×10^8 m/s	Mb/s	≤10 m
Acoustic	1,500 m/s	kb/s	km
Optical	3.33×10^8 m/s	Mb/s	
Communication paradigm	**Channel dependency**		**Stealth operation**
MI	Conductivity		Yes
EM	Conductivity, multipath		Yes
Acoustic	Multipath, Dropper, temperature, pressure, salinity, environmental sound noise		Audible
Optical	Light scattering, line-of-sight communication, ambient light noise		Visible

can easily penetrate mediums such as water, sediment layer, and rock. Therefore, MC enable many important applications.

In [5], the authors introduced MI technologies to a wireless sensor network for underground pipeline monitoring. This MC system can provide a low-cost and real-time leakage detection and localization technique for underground pipelines. The authors of [6] and [7] analyzed the performance of an MC system underwater to measure basic communication metrics, such as the signal-to-noise ratio, bit error rate (BER), connectivity, and communication bandwidth. An MC system can also be applied to address the issue of water shortage confronting irrigation, which was studied in [8]. The authors of [8] used the MC network for Wireless Underground Sensor Networks (WUSN) instead of the EM wave communication for WUSN to realize an irrigation control system in horticulture in Australia. In a district heating system, MC technologies also play a big role in coping with the challenging underground channel environment discussed in [9]. In addition, MC technologies can be of great benefits in rescuing people if there's a mining disaster, flooding, or a collapse of underground tunnels [10].

Besides the automation and communication applications presented above, another important application of MC technologies is localization. MI localization does not rely on a propagating wave but generates a quasi-static magnetic field in the air. This direction has drawn much attention recently. A team at the University of Oxford developed an MI-based localization system that is shown in Fig. 1.3 to provide 3D localization in [11]. This incrementally deployed system can quickly localize a challenging underground scenario with accuracy around 1 m. In [12], the MI system was applied to indoor localization. MI localization has a huge advantage that obstacles, such as walls, floors, and people, which heavily impact the performance of EM waves are almost "transparent" to the MC system. However, the MI system has its own drawback, i.e., it

https://doi.org/10.1017/9781108674843.003 Published online by Cambridge University Press

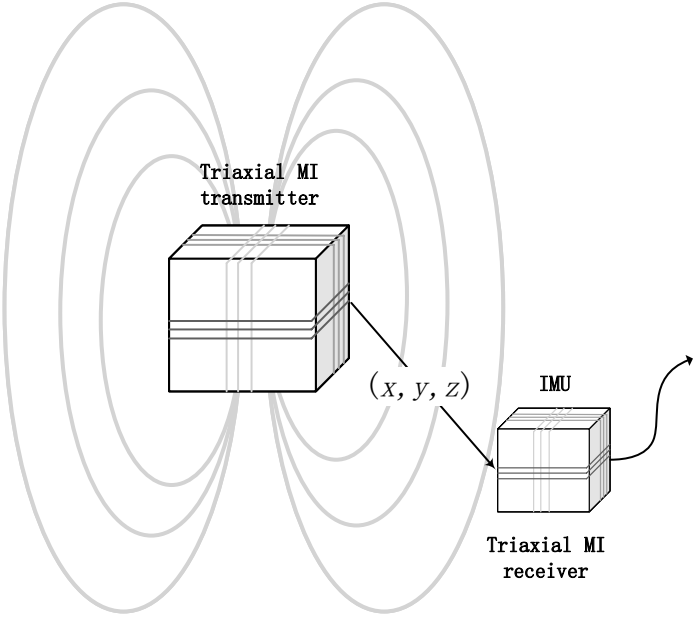

Figure 1.3 MI-based localization system

is sensitive to materials. By using signal processing and sensor fusion across multiple-system layers against the sensitivity to materials, the MI localization system can get 3D positioning with localization errors below 0.8 m even in some heavily distorted areas.

1.2 Preliminaries

1.2.1 Polar Coordinate

Polar coordinate has been frequently used in this book. As shown in Fig. 1.4, we use $\widehat{e}_r$, $\widehat{e}_\theta$, and $\widehat{e}_\phi$ to represent three unit coordinate vectors of a polar coordinate system. Let $\widehat{e}_x$, $\widehat{e}_y$, and $\widehat{e}_z$ be the unit coordinate vectors of a rectangular coordinate system. Then we have the following relationships:

$$\begin{aligned}
\widehat{e}_r \cdot \widehat{e}_z &= \cos\theta \\
\widehat{e}_\theta \cdot \widehat{e}_z &= \cos\theta + \frac{\pi}{2} \\
\widehat{e}_\phi \cdot \widehat{e}_x &= \cos\phi + \frac{\pi}{2} \\
\widehat{e}_\phi \cdot \widehat{e}_y &= \cos\frac{\pi}{2} - \phi.
\end{aligned} \tag{1.1}$$

https://doi.org/10.1017/9781108674843.003 Published online by Cambridge University Press

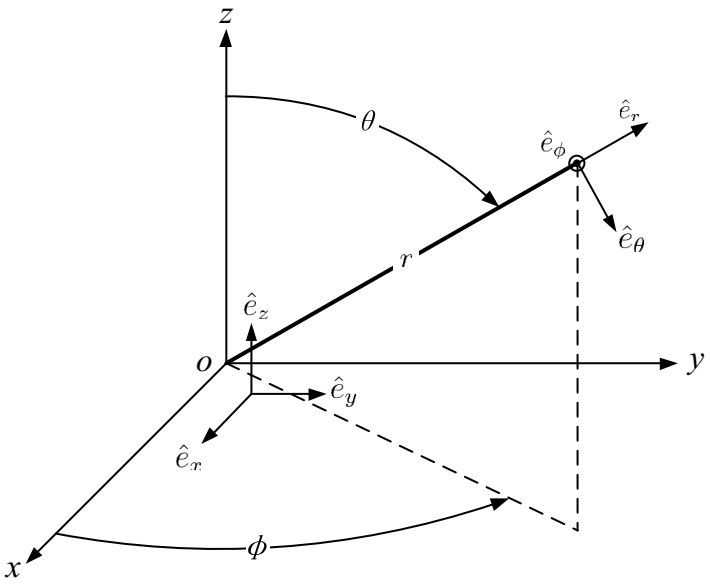

Figure 1.4 Polar coordinate and unit vectors

1.2.2 Loop Antenna

MC are accomplished with the use of loop antennas. A single-turn circular loop antenna is shown in Fig. 1.5 on the x–y plane at $z = 0$. Let a represent the radius of the coil. Let the wire is assumed to be very thin and the current $I = I_0$, where I_0 is a constant [13].

Then the radiated fields of such a loop antenna at an arbitrary point N_0 are approximately expressed under the spherical coordinates with the magnetic field components [13]:

$$\begin{aligned} H_r &= j\frac{ka^2 I_0 \cos\theta}{2r^2}\left[1+\frac{1}{jkr}\right]e^{-jkr} \\ H_\theta &= -\frac{(ka)^2 I_0 \sin\theta}{4r}\left[1+\frac{1}{jkr}-\frac{1}{(kr)^2}\right]e^{-jkr} \\ H_\phi &= 0, \end{aligned} \tag{1.2}$$

while the electric-field components [13]:

$$\begin{aligned} E_\phi &= \eta\frac{(ka)^2 I_0 \sin\theta}{4r}\left[1+\frac{1}{jkr}\right]e^{-jkr} \\ E_r &= E_\theta = 0, \end{aligned} \tag{1.3}$$

where $k = 2\pi/\lambda$.

The signal energy of MC is transmitted in a near-field region, i.e., $kr \ll 1$. With this assumption, the expressions of the fields given by (1.2) and (1.3) can be simplified as [34]:

https://doi.org/10.1017/9781108674843.003 Published online by Cambridge University Press

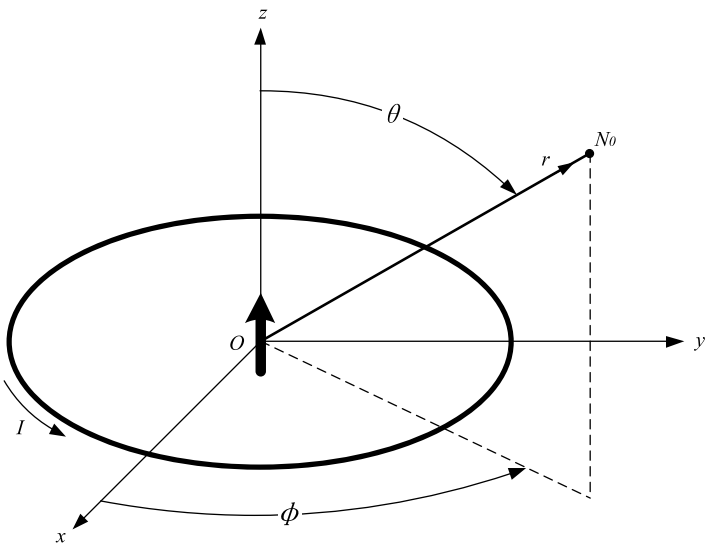

Figure 1.5 Circular loop antenna

$$\begin{aligned} H_r &\simeq \frac{a^2 I_0 e^{-jkr}}{2r^3} \cos\theta \\ H_\theta &\simeq \frac{a^2 I_0 e^{-jkr}}{4r^3} \sin\theta \\ H_\phi &= 0 \end{aligned} \tag{1.4}$$

$$\begin{aligned} E_\phi &\simeq -j\frac{a^2 k I_0 e^{-jkr}}{4r^3} \sin\theta \\ E_\theta &= E_r = 0. \end{aligned} \tag{1.5}$$

1.2.3 Magnetic Moment

Magnetic moment is a fundamental metric to measure the capacity of an MI loop antenna; it is measured by the following equation:

$$m = IA, \tag{1.6}$$

where A represents the area of loop. Additionally, in a standard circular loop, we have $A = \pi a^2$. In this case, the magnetic moment of a loop antenna of N turns is given by

$$m = NIA. \tag{1.7}$$

An MI antenna with a larger magnetic moment can radiate a stronger magnetic field signal.

In an MC system, the magnetic field is measured in the B-field with SI unit tesla (symbol: T). Considering a constant value of transmitting current I, we have the frequency $f = 0$ and $k = 0$, and consequently $e^{-jkr} = 1$. The magnetic field vector at the point N_0 (Fig. 1.5) in a uniform vacuum space is

https://doi.org/10.1017/9781108674843.003 Published online by Cambridge University Press

Table 1.2 Resistivity

Material	$\rho(\Omega\cdot$ m) at 20 °C
Carbon(graphene)	1×10^{-8}
Silver	1.59×10^{-8}
Copper	1.68×10^{-8}
Annealed copper	1.72×10^{-8}
Gold	2.44×10^{-8}
Aluminum	2.82×10^{-8}
Tungsten	5.6×10^{-8}
Iron	9.71×10^{-8}

$$\widehat{B} = \widehat{e}_r \frac{\mu_0 a^2 I_0 N}{2r^3} \cos\theta + \widehat{e}_\theta \frac{\mu_0 a^2 I_0 N}{4r^3} \sin\theta, \tag{1.8}$$

where $\mu_0 = 4\pi \times 10^{-7}$ T · m/A is the permeability of vacuum. Hence, the magnitude of $\widehat{B}$ is

$$\mathbf{B} = \left|\widehat{B}\right| \frac{\mu_0 NIA}{4\pi r^3} \sqrt{3\cos\theta^2 + 1} = \frac{\mu_0 m}{4\pi r^3} \sqrt{3\cos\theta^2 + 1}. \tag{1.9}$$

Equation (1.9) reveals that, for a given range r, the magnetic field strength is proportional to the magnetic moment m, while for a given receiving magnetic field strength threshold, the transmitting range $r \propto m^{1/3}$. We conclude that three ways can be applied to improve the magnetic field signal and the transmitting range from (1.9): enlarging the area A, adding loop turns N, and increasing transmitting current I. Although the three parameters A, N, and I are proportional to the magnetic moment, the consequent increases of consuming power are different.

The power consumed on the antenna loop is directly related with the current I, i.e., $P \propto I^2$. On the other hand, increases in the number of turns N and area A lead to the growth of the direct-current (DC) resistance. A fundamental way to calculate the DC resistance of a loop is Pouillet's law

$$R = \rho \cdot \frac{l_w}{A_w}, \tag{1.10}$$

in which ρ is the resistivity of the loop material, $l_w = 2\pi aN$ represents the total wire length, and A_w is the cross-sectional area of the wire. We provide the resistivity of some conductive materials in Table 1.2. Usually, the antenna loop is made of the wire following the American Wire Gauge (AWG) standard, whose resistance per length ranges from $2 \times 10^{-4}\Omega\cdot$ m^{-1} to $3\Omega \cdot$ m^{-1} with different wire diameter). Thus, we can use resistance per length to calculate the total DC resistance:

$$R = \rho_l l_w. \tag{1.11}$$

For a circular loop, $l_w = 2a \cdot \pi$.

After we figure out the calculation of antenna resistance, we can find that the number of turns N is proportional to the DC resistance. On the other hand, the loop area A is related to the circumference as well as the total length: $l_w \propto A^{0.5}$. Given that the

https://doi.org/10.1017/9781108674843.003 Published online by Cambridge University Press

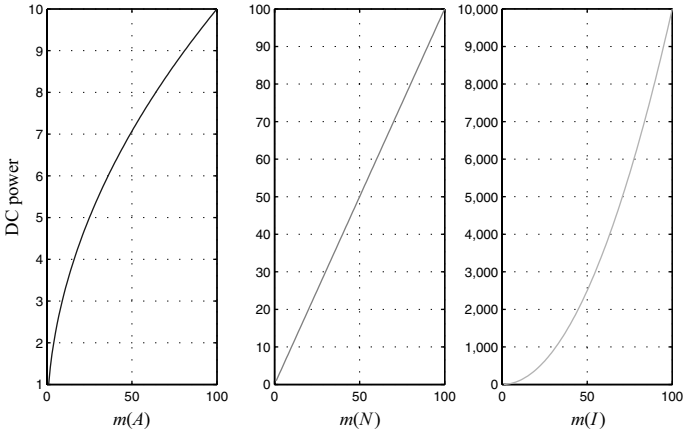

Figure 1.6 Normalized DC power and magnetic moments

power $P \propto R$, we conclude that enlarging the loop area A is the most efficient way to increase the magnetic moment. A normalized DC power versus magnetic moment is shown in Fig. 1.6. The magnetic moments vary from 1 to 100 times by changing A, N, and I, respectively.

It should be noted that only DC resistance and DC power are considered in this section; inductive resistance and conductive resistance in the case of alternating current (AC) will be discussed in Chapter 2. Static magnetic field strength can be treated as a fundamental measurement of the MI signal. The magnetic field sensitivity is a key parameter for a receiver, because advanced MC technologies are all based on the receiving of the magnetic field signal. However, the sensitivity performance of a receiver depends on the technologies of antenna design, antenna manufacturing, and receiving circuit, which is costly and empirical.

1.3 Mutual Inductance Circuit

In order to analyze the communication performance, a mutual inductance model is used as presented in Fig. 1.7. In this model, we take the signal frequency into consideration. This model is able to help us to figure out the power-transmitting process in MC. Similar to the wireless power transport, an MC channel evaluated by an electric voltage is characterized by the following equation:

$$\begin{aligned} Z_t &= R_t + j\omega L_t + \frac{1}{j\omega C_t}, \quad Z_t' = \frac{\omega^2 M^2}{R_r + j\omega L_r + \frac{1}{j\omega C_r} + Z_L} \\ Z_r &= R_r + j\omega L_r + \frac{1}{j\omega C_r}, \quad Z_t' = \frac{\omega^2 M^2}{R_t + j\omega L_t + \frac{1}{j\omega C_t}} \\ U_M &= -j\omega M \frac{U_s}{R_t + j\omega L_t + \frac{1}{j\omega C_t}}. \end{aligned} \tag{1.12}$$

https://doi.org/10.1017/9781108674843.003 Published online by Cambridge University Press

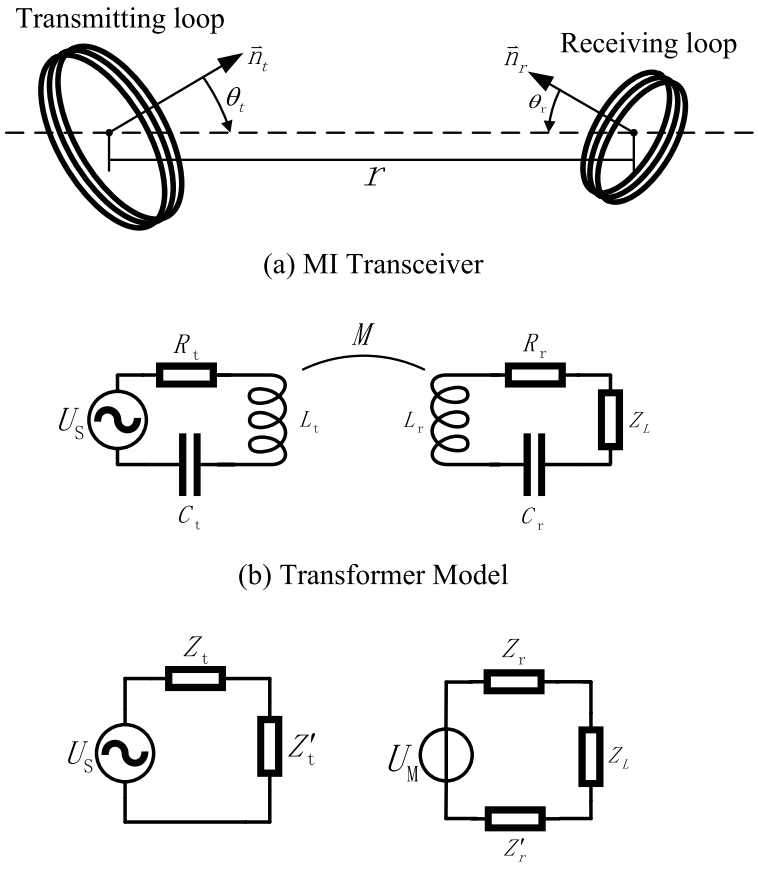

Figure 1.7 Equivalent mutual induction circuit

Here U_M is the induced voltage at the receiving side, which can further be used to derive the receiving power in Section 1.4, U_s is the source voltage at the transmitting side, R_t and R_r are the DC resistances of the transmitting loop and receiving loop, respectively, while L_t and L_r represent the inductance of transmitting and receiving coil, respectively. C_r and C_t are the capacitances that are decided by the resonant signal frequency given as follows:

$$C_r = \frac{1}{(2\pi f)^2 L_r}, \quad C_t = \frac{1}{(2\pi f)^2 L_t}. \tag{1.13}$$

1.3.1 Self-Inductance

According to the definition of inductance, we establish that a current I in the transmitting loop produces a magnetic flux Φ_B through the central region of the loop. With the flux known, the self-inductance is obtained as [14]

https://doi.org/10.1017/9781108674843.003 Published online by Cambridge University Press

$$L = \frac{N\Phi_B}{I}, \tag{1.14}$$

where L is the self-inductance, N is the number of loop turns, Φ_B is the magnetic flux, and I is the current.

The magnetic flux Φ_B is calculated as follows:

$$\Phi_B = nl\mathbf{B}A, \tag{1.15}$$

where l is the length near the middle of the loop, n is the number of turns per length, and A is the area of the loop. The magnitude

$$\mathbf{B} = \mu In, \tag{1.16}$$

where μ is the magnetic permeability of space medium, and from Eq. (1.14), we have

$$L = \frac{N\Phi}{I} = \frac{nL\mathbf{B}A}{I} = \mu n^2 lA. \tag{1.17}$$

For an ideal loop, when $n = N$ and l is set to $0.5a$ [15], the self-inductance of transmitting and receiving loop is

$$\begin{aligned} L_t &\simeq \frac{1}{2}\mu\pi N_t^2 a_t \\ L_r &\simeq \frac{1}{2}\mu\pi N_r^2 a_r. \end{aligned} \tag{1.18}$$

1.3.2 Mutual Inductance

Similar to the calculation of self-induction, we assume that the current I produces a magnetic flux Φ_r through the receiving loop. The mutual inductance of the two loops in Fig. 1.7 is then obtained as

$$M = \frac{N_r\Phi_r}{I}. \tag{1.19}$$

Since the mutual inductance is defined under a static situation, we use equation (1.8) to calculate the magnetic flux Φ_r:

$$\begin{aligned} \Phi_r &= \widehat{B} \cdot \overrightarrow{n}_r \cdot A_r \\ &= \left(\widehat{e}_r \cdot \overrightarrow{n}_r \cdot 2\cos\theta_t + \widehat{e}_{\theta_t} \cdot \overrightarrow{n}_r \cdot \sin\theta_t\right) \frac{\mu a_t^2 I N_t}{4r^3} A_r \\ &= \left(2\cos\theta_r \cos\theta_t + \sin\theta_r \sin\theta_t\right) \frac{\mu\pi a_t^2 a_r^2 I N_t}{4r^3}. \end{aligned} \tag{1.20}$$

As a result, we have

$$M = \mu\pi N_t N_r \frac{a_t^2 a_r^2}{4r^3}(2\sin\theta_t \sin\theta_r + \cos\theta_t \cos\theta_r). \tag{1.21}$$

1.3.3 Skin Effect

Because of the changes in the magnetic field, MC are influenced by the skin effect [16]. The alternating magnetic field of the MI system caused an alternating electric current

https://doi.org/10.1017/9781108674843.003 Published online by Cambridge University Press

to become distributed with a conductive material, and the electric current flows mainly between the outer surface and a level called the skin depth, δ. The skin effect can be ignored if the operating frequency is low, because the skin depth is very large and the consequent EM field existed anywhere in the medium [16]. However, for the MI system with a high carrier frequency of up to tens of megahertz [15, 17], δ becomes much smaller, and the EM field has enough strength within a short range around the MI loop, which significantly weakens the mutual induction between antenna loops.

In order to model the influence of skin effect, we introduce an addition attenuation factor G to the mutual inductance [16]. The addition attenuation factor G is a function of distance r between the antenna loops and the skin depth δ in the medium. According to the model proved in [18], we have

$$G(r,\delta) = \left| \int_0^{\infty} \frac{x^3}{x + \sqrt{x^2 + j(\frac{\sqrt{2}r}{\delta})^2}} e^{\sqrt{-x^2 - j\frac{\sqrt{2}r}{\delta}}} \cdot dx \right|. \tag{1.22}$$

Let ϵ and σ represent the medium permittivity and conductivity, respectively; then the skin depth δ can by calculated by [19]

$$\delta = \frac{1}{2\pi f \sqrt{\frac{\mu}{\epsilon}\left(\sqrt{1 + \frac{\sigma^2}{(2\pi f)^2\epsilon^2}} - 1\right)}} \approx \sqrt{\frac{1}{\pi f \mu \sigma}}. \tag{1.23}$$

Although the skin effect is accurately characterized by $G(r,\delta)$, equation (1.22) is not favorable in most applications. Therefore, it has been approximated based on a numerical method by an exponential function $\frac{r}{\delta}$ in [16]:

$$G \simeq 1.004 \cdot e^{-0.1883 \cdot (\frac{r}{\delta})^{1.671}}. \tag{1.24}$$

For the MC channel, the skin effect leads to a decline in the mutual induction between two antenna coils expressed as follows:

$$M = G \cdot \mu\pi N_t N_r \frac{a_t^2 a_r^2}{4r^3}(2\sin\theta_t \sin\theta_r + \cos\theta_t \cos\theta_r). \tag{1.25}$$

1.3.4 Environment Medium

The MI signal penetrates an underground and underwater lossy medium much more efficiently than EM waves [20]. However, the impact of the medium is non-ignorable. Existing MI research is mainly based on a simple environment, such as a single uniform medium space or an underwater environment with surface reflection and lateral waves [20]. Statistical channels for a complex environment like a Rayleigh fading channel are lacked.

Conductivity

Conductivity measures a material's ability to conduct an electric current. It is commonly represented by the Greek letter σ. The conductivity of a material often varies

https://doi.org/10.1017/9781108674843.003 Published online by Cambridge University Press

Table 1.3 Conductivity

Material	Conductivity $\sigma(S/m)$ at 20 °C
Carbon (graphene)	1.00×10^{8}
Copper	5.96×10^{7}
Aluminum	3.50×10^{7}
Calcium	2.98×10^{7}
Sea water	4.80
Drinking water	5.00×10^{-4} to 5.00×10^{-2}
Deionized water	5.50×10^{-6}
Silicon	1.56×10^{-3}
Air	3.00×10^{-15} to 8.00×10^{-15}

Table 1.4 Permeability

Material	Permeability $\mu(H/m)$	Relative permeability $\frac{\mu}{\mu_0}$
Vacuum	$4\pi \times 10^{-7}(\mu_0)$	1
Air	$1.25663753 \times 10^{-6}$	1.00000037
Water	1.256627×10^{-6}	0.999992
Concrete (dry)	$4\pi \times 10^{-7}$	1
Aluminum	1.256665×10^{-6}	1.000022
Platinum	1.256970×10^{-6}	1.000265
Wood	1.2566376×10^{-6}	1.00000043
Copper	1.256629×10^{-6}	0.999994

with different factors, including temperature, purity, and concentration of water that contains dissolved salts (the conductivity of some common materials can be found in Table 1.3). In a radio frequency (RF)-challenged environment, the transmission medium is mostly a nonconductive material. However, there can be a nonnegligible level of conductivity due to humidity and mineral substances.

Permeability

Determining the permeability of a coal mine is a complex problem; the relative permeability of coal to gas and water depends on the nature of gas, the operational pressure, and fluid–mineral interactions (the permeability of other common materials can be found in Table 1.4 for reference).

1.3.5 Metamaterial

Metamaterials for EM waves have unusual physical features, such as the negative refraction index, including permittivity ε and permeability μ. To achieve a certain refractive index, metamaterials are carefully built to have a smaller structure feature than the wavelength of the respective EM wave. A negative refraction index is an important characteristic of metamaterials to distinguish them from natural existing materials as illustrated in Fig. 1.8.

https://doi.org/10.1017/9781108674843.003 Published online by Cambridge University Press

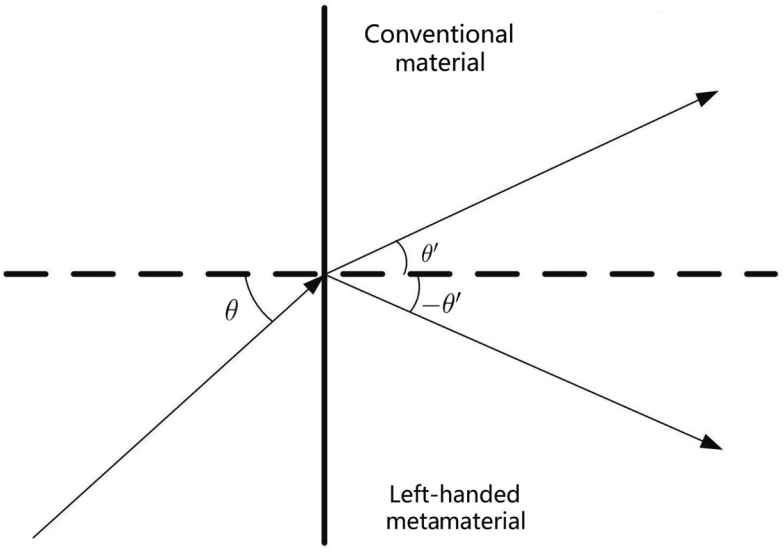

Figure 1.8 Negative refractive index of metamaterial

Application of Metamaterials

Metamaterials are widely used in different kinds of fields. For example, MRI can be enhanced using metamaterials. Long-Term Evolution (LTE) handsets deploy metamaterials for antenna array. Metamaterials can also be deployed in magnetic communications to enhance both the wireless communications using point-to-point MI and MI waveguide. Compared to EM wave-based communication, MI can easily penetrate the lossy medium in RF-challenging environments. One major drawback is the limited transmission distance due to the fast attenuation of magnetic fields. The techniques to enhance magnetic fields using metamaterials will be discussed later.

1.3.6 Waveguide Structure

The transmission distance of an MI system suffers from fast path loss despite its relatively stable channel condition compared to the EM wave. To this end, a waveguide structure using several passive relay devices is employed. The relay point is usually a simple coil that induces a sinusoidal current in the next coil and so on until it passes to the receiver node. Hence, the relay point needs no energy sources or processing devices. The waveguide system is illustrated in [17] and the equivalent circuit diagram of which is shown in Fig. 1.9.

We assume that the waveguide structure uses the same type of coils with the same parameters. To be specific, we let L be the coil self-induction, M be the mutual inductance between adjacent coils, U_t be the voltage of the transmitter energy source, R be the copper resistance of the coil, C be the capacitor loaded in each coil, and Z_L be the load impedance of the receiver. There are totally $(k-1)$ passive relays that are placed equidistantly between the transceivers.

https://doi.org/10.1017/9781108674843.003 Published online by Cambridge University Press

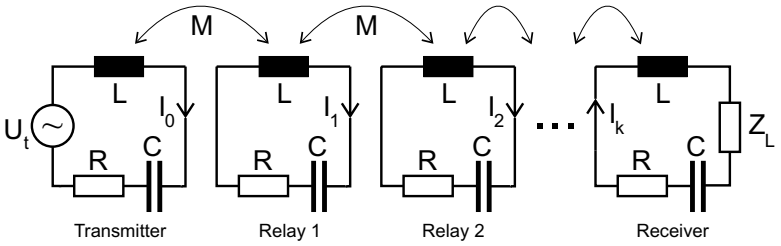

Figure 1.9 Block diagram of an MI waveguide with a transmitter, a receiver, and $(k-1)$ relays

The path loss function is given by

$$L_p(f) = \frac{|S(x,x_L,k)\cdot S(x,x_L,k+1)|}{|Im\{x_l\}|}, \tag{1.26}$$

where f is the signal frequency and j is the imaginary unit, with $x_L = \frac{Z_L}{j2\pi fM}$ and $x_L = \frac{Z}{j2\pi fM}$, and

$$S(x,x_L,n) = F(x,n) + x_L \cdot F(x,n-1), \tag{1.27}$$

with

$$F(x,n) = \frac{\left(\frac{x+\sqrt{x^2-4}}{2}\right)^{n+1} - \left(\frac{x-\sqrt{x^2-4}}{2}\right)^{n+1}}{\sqrt{x^2-4}}. \tag{1.28}$$

The load impedance is matched only to the equivalent impedance Z_e at the carrier frequency using a resistor, i.e.,

$$Z_L = Z_{L,R} = Re\left\{j2\pi f_0 M \cdot \frac{F(x_0,k+1)}{F(x_0,k)}\right\}. \tag{1.29}$$

1.4 MI Communication Performance

1.4.1 Received Power

MC is a near-field technique where communication is achieved by coupling in the non-propagating near-field. The radiation resistance in MC is so small that the radiation power can be neglected. Therefore, the induced power consumed at the MI receiver is the major power consumption. The transmitting power of the MI system consists of the induced power consumed at the MI receiver and the power consumed in the coil resistance. If the antenna impedance is very small, the ratio of the received energy to the propagation energy is 1 because the propagation energy and the received energy are consistent with the distance variation. The advantage of MC is that most of the energy in this technique is delivered to the receiver, and limited energy propagation is wasted in the surrounding environment. Using the circuit model in Fig. 1.7, the transmitted power P_t of the primary coil and the received power P_r are given as follows:

https://doi.org/10.1017/9781108674843.003 Published online by Cambridge University Press

$$\begin{aligned} P_t(r) &= \left| \frac{U_s^2}{Z_t + Z_t'} \right| \\ &= \frac{U_s^2}{\left| \frac{C_t M^2 \omega^2}{\frac{1}{jC_t w} + jL_t\omega + R_t} + \frac{1}{jC_t\omega} + jL_t\omega + R_t \right|} \\ &= \left| \frac{M^2\omega^2}{\frac{1}{jC_t\omega} + jL_t\omega + R_t + Z_L} + \frac{1}{jC_t\omega} + jL_t\omega + R_t \right| I_t^2, \end{aligned} \tag{1.30}$$

$$\begin{aligned} P_r(r) &= \left| \frac{Z_L \cdot U_M^2}{(Z_L + Z_r + Z_r')^2} \right| \\ &= \frac{M^2 U_s^2 \omega^2 Z_L}{\left| \frac{1}{jC_t\omega} + jL_t\omega + R_t \right|^2 \left| \frac{M^2\omega^2}{\frac{1}{jC_r\omega} + R_r + j\omega L_r + Z_L} + \frac{1}{jC_r\omega} + jL_r\omega + R_r + Z_L \right|^2} \\ &= \frac{1}{2} \frac{|j\omega M|^2 Z_L}{\left| j\omega L_r + \frac{1}{j\omega C_r} + R_r + Z_L \right|^2} I_t^2, \end{aligned} \tag{1.31}$$

where I_t is transmitting current. In the case that MC work at the resonance frequency ($\omega = \omega_0$), $j\omega L_t + 1/jwC_t = 0$, $j\omega L_r + 1/jwC_r = 0$, and $Z_L = R_r$, the transmitted power and the received power are obtained as

$$P_t = \left(\frac{\omega_0^2 M^2}{R_t + R_r} + R_t \right) I_t^2 \tag{1.32}$$

$$P_r = \frac{\omega_0^2 M^2}{4R_r} I_t^2. \tag{1.33}$$

1.4.2 Path Loss

Path loss is the reduction in the power density (attenuation) of an EM wave as it propagates through space or media. It is also a major component in the analysis and design of an MI system. As the distance increases, the receiver will receive less and less energy because of *path loss*. It should be noted that the power is not really lost but not transmitted. The path loss of the MI system with a transmission distance is defined as

$$L_{\mathrm{MI}}(r) = -10 \lg \frac{P_r(r)}{P_t}, \tag{1.34}$$

where "lg" denotes "$\log_{10}$," $P_r(r)$ is the received power at the receiver that is r meters away from the transmitter and satisfy (1.31), and $P_t(r_0)$ is the reference transmitting power when the transmission distance is a very small value and can be looked as (1.30). In what follows, we will discuss the commonly used scenarios.

Under the scenarios of high operating frequency ($R_t \ll \omega\mu$, $R_r \ll \omega\mu$) and considering that r_0 is adequately small, $P_t(r_0) \simeq U_s^2/R_t$. The path loss of the MC system is simplified as

https://doi.org/10.1017/9781108674843.003 Published online by Cambridge University Press

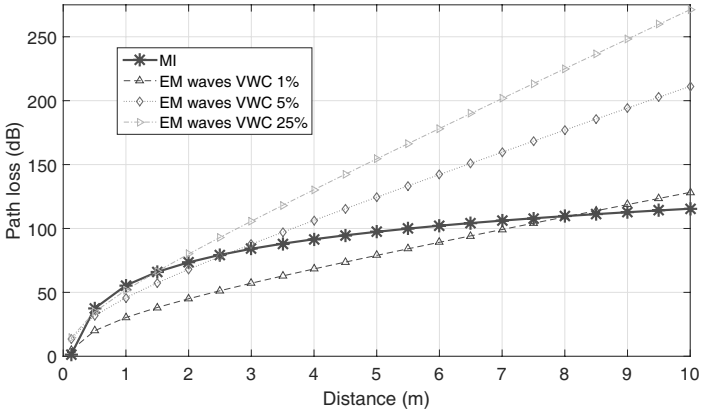

Figure 1.10 Path loss of the EM wave system and that of the MI system with different soil water content

$$\begin{aligned} L_{\mathrm{MI}}(r) &= -10\lg\frac{P_r(r)}{P_t(r_0)} = -10\lg\frac{N_r a_t^3 a_r^3}{4N_t r^6} \\ &= 6.02 + 60\lg r + 10\lg\frac{N_t}{N_r a_t^3 a_r^3}. \end{aligned} \tag{1.35}$$

The path loss of the MI system and that of the EM wave system are evaluated using MATLAB. For the MI system, the operating frequency f is set to 10 MHz, i.e., $\omega = 2\pi f = 2\pi \times 10^7$; the transmitter and the receiver coils have the same number of turns 5 ($N_t = N_r = 5$) and radius ($a_t = a_r = 0.15$ m). The coil is made of the copper wire with 1.45-mm diameter and with the resistance of unit length $R_0 = 0.01\ \Omega$/m. For the EM wave system, the operating frequency is set to 300 MHz. The permeability of the underground transmission medium is the same as that in the air, which is $4\pi \times 10^{-7}$H/m. In Fig. 1.10, the path loss of the MI system and that of the EM wave system are shown in dB versus the transmission distance with different soil volumetric water content (VWC). It is interesting to see that, compared with the path loss of the EM wave system, the path loss of the MI system is less affected by the earth layer since the permeability is almost unchanged. Therefore, the MI system can achieve smaller path loss than the EM wave system after a sufficient long transmission distance even in the very dry soil medium, which makes MC a promising wireless technology for underground environments.

Let's now consider the scenarios where the operating frequency is low and all antennas of transceivers are identical. Suppose that the resistance of the transmitter and that of the receiver have the same value R, and the MI system works at a resonance frequency ω that is approximately equal to the resonance angular frequency ω_0. According to (1.32) and (1.33), the path loss L_{MI} is then obtained as

$$L_{\mathrm{MI}}(r) = 10\lg\frac{2(2R^2 + \omega_0^2 M^2)}{\omega_0^2 M^2} \approx 10\lg\frac{4R^2}{\omega_0^2 M^2}. \tag{1.36}$$

https://doi.org/10.1017/9781108674843.003 Published online by Cambridge University Press

1.4.3 Bit Error Rate and Communication Range

BER is the number of bit errors per unit time. It may be affected by transmission channel noise, interference, distortion, attenuation, wireless multipath fading, etc. Owning to the quasi-static channel of MC, the BER characteristic depends mainly on three factors: the path loss, the noise level, and the modulation scheme used by the system. When the signal level remains the same, the noise level is inversely proportional to the signal-to-noise ratio (SNR), which can be calculated by SNR $= P_t - L_{\mathrm{MI}} - P_n$, where P_t is the transmitting power and P_n is the average noise level. The modulation scheme is an important factor influencing the BER. For example, in the case of QPSK and 2PSK modulation in the AWGN channel, the BER as a function of the SNR is given by BER $= \frac{1}{2}\mathrm{erfc}(\sqrt{\mathrm{SNR}})$, where $\mathrm{erfc}(\cdot)$ is the error function.

When BER of the MI link between the transmitter and the receiver increases above a threshold ($\mathrm{BER_{th}} = 1\%$), the communication can be looked as invalid if there are lots of error data that cannot be corrected. Now that the path loss L_{MI} is the function of distance (r) as depicted in (1.35), the fact that the SNR is in relationship with the distance results in BER $= \mathrm{BER}(r)$. Therefore, the communication range $r_{\max}$ satisfy

$$\frac{1}{2}\mathrm{erfc}(\sqrt{P_t - L_{\mathrm{MI}}(r_{\max}) - P_n}) = 0.01. \tag{1.37}$$

Equation (1.37) exhibits that the communication range increases with the increase of $\frac{P_t}{P_n}$. As described in Fig. 1.11, where we set P_t as 10 dBm, the transmission range of the MI system is always larger than the EM wave system in a low noise scenario. However, in the high noise scenario, the transmission range of the MI system is between the range of the EM wave system in dry soil and the system in wet soil.

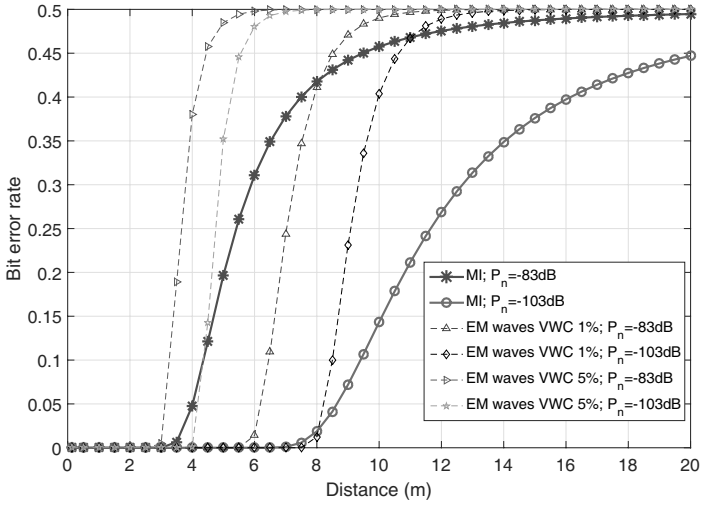

Figure 1.11 Bit error rate of the MI system and the EM wave system with different soil water content and noise level

https://doi.org/10.1017/9781108674843.003 Published online by Cambridge University Press

In practical applications, the operating frequency must be low enough to ensure communicating in the near-field range. For example, we suppose that the operating frequency $f = 10$ kHz, the transmitting power $P_t = 40$ dBm, and the coils of the receiver and the transmitter are identical, the radius $r = 4$ m, and the number of each coil $N = N_t = N_r = 12$. According to (1.37) and (1.36), the propagation distance will be above 600 m.

1.5 Channel Capacity

Despite the numerous advantages, the channel capacity of MC is the primary concerns. With reason that the MI transceivers always work at resonance frequency to ensure the low path loss, the bandwidth of the MI-based channel is much smaller than that of the EM wave-based channel. The narrow bandwidth results in the low capacity. According to the Shannon theorem, the capacity is proportional to the bandwidth and the logarithm of SNR at the receiver. The SNR of the MI system has been introduced in Section 1.4, and the bandwidth will be introduced in the following section.

1.5.1 Bandwidth

The fractional bandwidth of an MI system can be estimated from the loaded quality factors of the transmitter and the receiver by

$$B_w = \begin{cases} \frac{f_0}{Q_1}, & Q_1 > Q_2 \\ \frac{f_0}{Q_2}, & Q_1 < Q_2, \end{cases} \tag{1.38}$$

where f_0 is the resonance frequency, and $Q_1 = \frac{\omega L_r}{R_t + R_r}$ and $Q_2 = \frac{\omega L_r}{R_r}$ are the loaded quality factors of transceivers, respectively. The bandwidth of the MI system can be improved by increasing the resistance and decreasing the self-inductance of the coils.

At this resonance frequency, all the coils can achieve the resonance. However, if a deviation from the resonance frequency occurs, each coil will not achieve the resonant status and the load at the receiver will not match that of the system, and the path loss will increase. As a result, the 3-dB bandwidth B_{MI} is adopted as the MI channel bandwidth. The 3-dB bandwidth can be obtained from the following equation:

$$L_{\mathrm{MI}}\left(f_0 + \frac{1}{2}B_{\mathrm{MI}}\right) - L_{\mathrm{MI}}(f_0) = 3\mathrm{dB}. \tag{1.39}$$

When the transmitter and the receiver have the same number of coils, the 3-dB bandwidth of the MI system is

$$B_{\mathrm{MI}} = \frac{R\left(\sqrt{2}-1\right)}{\mu\pi^2 a N^2}. \tag{1.40}$$

For example, when the operating frequency is 10 MHz, the 3-dB bandwidth of the MI system is around 2 KHz. The bandwidth is not affected by the transmission distance. We can notice that the 2-kHz bandwidth of the MI system is much smaller than that of the EM wave system. The small bandwidth results in the low communication data rate.

https://doi.org/10.1017/9781108674843.003 Published online by Cambridge University Press

1.5.2 Channel Capacity

The capacity of a digital MI system is defined in the light of Shannon's information theory and given by

$$C_a = \int_{f_0-\frac{B_{\mathrm{MI}}}{2}}^{f_0+\frac{B_{\mathrm{MI}}}{2}} \log\left(1+\frac{P_t(f)L_{\mathrm{MI}}(f)}{P_n}\right), \tag{1.41}$$

where f_0 denotes the resonant frequency, and $f_0 = \frac{1}{2\pi\sqrt{LC}}$, L_{MI} is the path loss of the MI system, P_n is the noise power spectral density, and $P_t(f)$ is the power spectral density of transmit.

The composition of the noise factor includes the external noise and the internal noise. The external noise includes background noise, and co-channel and adjacent channel interference, which has the average power $P_{n,e}$. The internal noise $P_{n,Z_{L,R}}(f)$ is often generated by an amplifier circuit. The internal noise can be simplified as the well-known Johnson-noise power spectral densities $\mathrm{E}\{P_{n,Z_{L,R}}(f)\} = 4KTR$, where $K = 1.38\times10^{-23}$ J/K is the Boltzmann constant, T is the temperature in Kelvin, R is the copper resistance in (2), and $\mathrm{E}\{\cdot\}$ denotes the expectation value. In general, the external noise is often between -70 and -110 dBm, and accordingly, $P_{n,e} \gg E\{P_{n,Z_{L,R}}(f)\}\cdot B_{\mathrm{MI}}$.

1.6 Network Connectivity

Apart from the analysis of the MI channel that characterizes the point-to-point performance, in this section, we focus on MI-based networks and start from a fundamental network property: connectivity.

Organized in different types of networks, MI networks can provide required facilities in corresponding scenes. For example, the personal emergency device system provided by the MST company is a one-way downward broadcast network, the primary use of which is to provide a mine-wide emergency messaging and alert system; the Senor network consisted of small MI nodes is organized in an ad-hoc network [15], which has the abilities to gather information from diverse physical phenomena and spread control signals.

Before embarking on the detailed analysis of the MI network connectivity, we introduce several fundamental problems in connectivity analysis in this section. The problems provided in the followings help one understand the framework of connectivity and can be used and extended in MI networks.

1.6.1 System Model

In this part, we introduce two basic factors in the formation of a wireless network. A wireless link describes the connection behavior for an arbitrary node pair, while node deployment decides the location distribution of all nodes in the network. Both factors have important effect on the network connectivity.

https://doi.org/10.1017/9781108674843.003 Published online by Cambridge University Press

Wireless Link

A wireless link between two nodes is decided by whether both of them can reach the other with its wireless signal. The transmission of a wireless signal is mainly influenced by a distance-dependent power decay, along with other effects, including shadowing, fading, polarization gain, *etc*., therefore, we model the wireless link between a node pair χ_n as follows:

$$P_{\chi_n} = \Phi(\chi_n). \tag{1.42}$$

Here P_{χ_n} denotes the probability that the two nodes in χ_n have a connection with each other, Φ is a function of the displacement of two nodes which includes the effects of distance, environments, and polarization.

A basic wireless link model is a uniform range model, which assumes that the signal power decay is only related to the distance. Let r_{χ_n} denote the distance between a node pair χ_n; then the uniform range model is described by the following equation:

$$P_{\chi_n} = \begin{cases} 0 & r(\chi_n) > r_0 \\ 1 & r(\chi_n) \le r_0 \end{cases}, \tag{1.43}$$

where $r(\chi_n)$ is the distance between the node pair and r_0 represents the maximal distance for signal receiving.

For MC, both transmitting and receiving signals have the polarization effect based on the angle between the transmitter and the receiver. Thus, we conclude a basic wireless link model of an MI model as follows:

$$P_{\chi_n} = \begin{cases} 0 & r(\chi_n) > r(f_\theta) \\ 1 & r(\chi_n) \le r(f_\theta) \end{cases}. \tag{1.44}$$

Here the polarization function f_θ depends on the antenna types as well as the specific channel models for given scenarios.

Node Deployment

Besides the node-to-node wireless link, the connectivity performance of the wireless network also depends on the Euclidean distribution of nodes. For large-scale wireless networks, the stochastic geometry-based point process provides a way of estimating the graphic characteristics of the network. The node deployment of the wireless network is assumed either to be deterministic, as the two examples shown in Figs. 1.12(a) and (b), or stochastic as shown in Figs. 1.12(c).

It has been proven that the random point process is a generally effective approach to describe the positions of wireless ad hoc networks [174]. Recalling that the MI

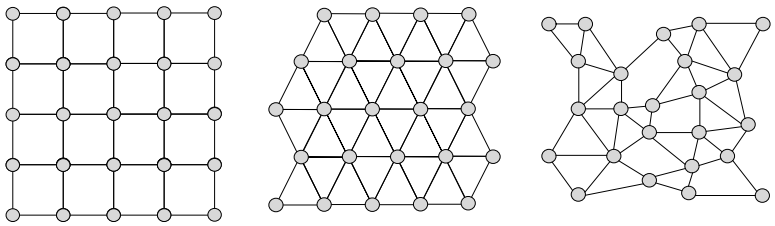

Figure 1.12 Deployment model

https://doi.org/10.1017/9781108674843.003 Published online by Cambridge University Press

networks are proposed for complex environments, which means that the available locations for node deployment are also randomly distributed. As a result, we continue to use the random point process to model the node deployment of the MI network.

The Poisson point process (P.P.P.) is a commonly used deployment model; a homogeneous P.P.P. is defined by the following two properties.

(a) The number of nodes U_d in each finite subspace $\mathbf{D}$ with a size of $\|\mathbf{D}\| = D$ follows a Poisson distribution, i.e.,

$$P(n \text{ nodes in } \mathbf{D}) = P(U_d = n) = \frac{\lambda^n}{n} e^{-\lambda};\ n \in \mathbf{N}_0, \tag{1.45}$$

where $\lambda = \rho D$ represents the expectation $\mathbf{E}\{U_d\}$ and $\mathbf{N}_0$ is the set for positive integers.

(b) The number of nodes N_j in disjoint spaces $\mathbf{D}_j, j \in \mathbf{N}_0$, is an independent random variable, i.e.,

$$P(N_1 = n_1 \bigcap N_2 = n_2 \bigcap \ldots \bigcap N_k = n_k) = \prod_{j=1}^{k} P(N_j = n_j). \tag{1.46}$$

Node Degree

Node degree is the number of neighbors of a node which it can communicate with. Depending on the wireless link mode and node deployment, one can derive the node degree of a certain type of network. The average node degree in a network is an essential factor in the following network connectivity analysis. For a randomly deployed network or nodes with a random wireless link, a node degree is expected.

1.6.2 Connectivity Analysis

Connected Probability

A connected network means that every node in a given network is connected to a single main component (Fig. 1.13) in a way that they can communicate with any other nodes

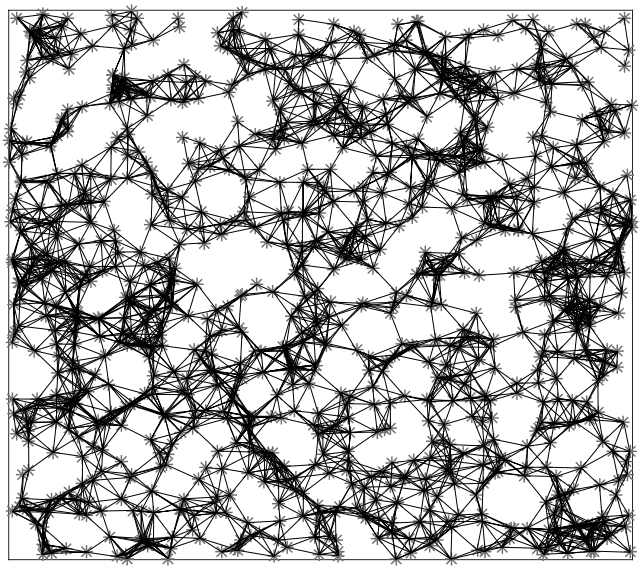

Figure 1.13 Connected large-scale wireless network

https://doi.org/10.1017/9781108674843.003 Published online by Cambridge University Press

in that network. Let **P**(con) denote the probability of a network to be connected. By analyzing the relationship of **P**(con) with the network conditions, including the node number and transmitting power we can find a proper way to establish an effective wireless network in applications. However, if the nodes in a network are randomly deployed as introduced in (1.6.1), it is impossible to find a condition such that the network is surely connected, i.e., **P**(con) = 1. Since for random node deployment, the probability for a node to have no neighbor is always positive, we, therefore, use a critical point **P**(con) = 0.99 to find the network conditions that make the network *almost-surely* connected.

A more general model for the measurement of a connected network is the *k*-connected network that is defined as follows. There are k independent paths for each node pair in the network to be connected. A connected network is at least 1-connected as shown in Fig. 1.14(b) while an example of 2-connected network is shown in Fig. 1.14(c). Network with a higher *k* has better connectivity, less congestion, and higher robustness.

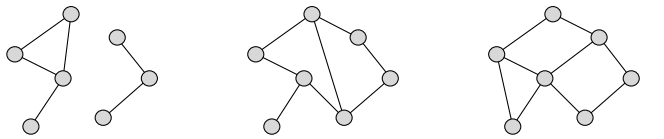

Figure 1.14 *k*-connectivity

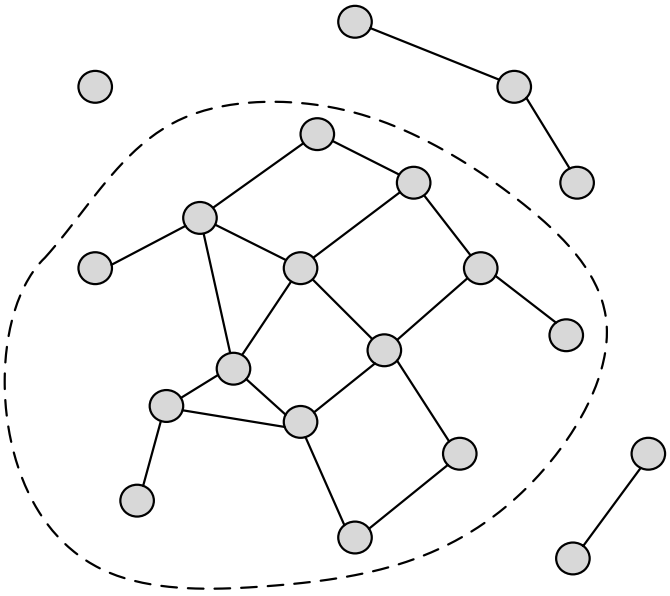

Figure 1.15 Giant component

https://doi.org/10.1017/9781108674843.003 Published online by Cambridge University Press

Giant Component

A giant component of a network is also used to measure a network connectivity. As shown in Fig. 1.15, a giant component is the biggest component in a network that contains the most nodes. By deriving the percentage of the giant component versus the whole network based on the network conditions, one can determine whether the network is connected. A high percentage (close to 1) of a giant component is also a commonly used condition in connectivity analysis.

https://doi.org/10.1017/9781108674843.003 Published online by Cambridge University Press